Nuclear Physics B289 (1987) 628–644
North-Holland, Amsterdam

CHROMOMAGNETIC ENERGY OF SU(2) GAUGE FIELDS ON A TORUS[†]

T.H. HANSSON[1], Pierre van BAAL[2,*] and I. ZAHED[1]

[1] *Nuclear Theory Group, Physics Department, State University of New York at Stony Brook, Stony Brook, New York 11794, USA*

[2] *Institute for Theoretical Physics, SUNY, Stony Brook, NY 11794, USA*

Received 17 July 1986

Inspired by the Savvidy-Copenhagen vacuum picture, we present a calculation of the chromomagnetic energy of pure SU(2) gauge fields defined on a torus. We avoid the perturbative instability of the Savvidy state by introducing magnetic flux through 't Hooft's twisted boundary conditions. The energy as a function of magnetic flux and volume is calculated to two-loop order. Nonperturbative effects related to tunneling processes are briefly discussed. We consider this calculation as a first step in a program aimed at exhibiting possible instabilities of the perturbative vacuum.

1. Introduction

Low energy hadron phenomenology using QCD based models, high-Q^2 jet physics, and numerical simulations using lattice cutoff and Monte Carlo techniques, all indicate that QCD correctly describes the strong interaction. It is a commonly accepted conjecture that the infrared singularities encountered in perturbation theory are cut off by nonperturbative effects that give rise to color confinement and chiral symmetry breaking [1].

Monte Carlo calculations based on a lattice regularization have been successfully used to obtain predictions from QCD using only the scale parameter as input. We do believe, however, that analytical methods are equally necessary in order to understand the physical mechanism behind the nonperturbative effects. It is fair to say that almost all analytical approaches are based on assuming an instability of the perturbative vacuum. We can mention the various variational approaches [2], the saddle point approximations around instantons [3], monopoles [4] or constant chromomagnetic fields [5], and the glueball condensate picture [6]. To establish the presence of such an instability (often referred to as "condensation") in an unam-

[†] Supported in part by the US Department of Energy under contract no. DE-AC02-76ER13001 and the National Science Foundation under grant no. DMS-84-05661.

*Address after September 1: CERN, CH-1211, Geneva 23, Switzerland.

biguous and calculable way, is obviously an important step towards a better understanding of nonperturbative QCD.

In this work we combine the ideas of the Savvidy-Copenhagen vacuum [5,7] with the techniques used to describe Yang-Mills fields on a torus [8], to develop a framework for studying chromomagnetic instabilities.

This paper is organized as follows. In sect. 2 we briefly discuss the Copenhagen vacuum and argue that the analysis on the torus is a good alternative. Sect. 3 gives the one-loop result for the vacuum energy as a function of volume and magnetic flux (for convenience we restrict ourselves to SU(2) and symmetric tori), and sect. 4 contains the corresponding two-loop calculation for nonzero magnetic flux. In sect. 5, we outline the use of a nonlocal gauge fixing procedure, that allows us to extend the calculation to zero magnetic flux. Sect. 6 describes various nonperturbative contributions related to tunneling, and in passing we also give the glueball mass to lowest order in the coupling constant for tori with nonzero magnetic flux. We conclude with some speculations about possible chromomagnetic instabilities of the perturbative vacuum.

2. Removing the perturbative instabilities

The so called Savvidy vacuum [5] is based on a (strong) background chromomagnetic field. Because of the strong color Zeeman effect, this state is energetically favoured over the perturbative vacuum. Early on, however, it was realized by Nielsen and Olesen [7] that this state is perturbatively unstable. They went on to demonstrate, that by exciting the "unstable mode" (or tachyon) in a periodic structure, the energy density could be lowered even further. Because of the periodicity it was not too surprising that the configurations found in the Copenhagen vacuum satisfied 't Hooft's twisted periodic boundary conditions [8]. To be specific, the so called ϑ_3 configurations, which minimize the energy within the ansatz based on the tachyonic mode, satisfy twisted boundary conditions in the (x, y) plane and are independent of z [9]. If we introduce periodic boundary conditions in the z-direction as well, the Copenhagen ansatz becomes equivalent to a gauge field configuration on the torus.

The twisted boundary conditions are given by,

$$A_k(\boldsymbol{x}+\boldsymbol{a}^{(j)}) = \Omega_j(\boldsymbol{x}) A_k(\boldsymbol{x}) \Omega_j^{-1}(\boldsymbol{x}) - i\Omega_j(\boldsymbol{x}) \partial_k \Omega_j^{-1}(\boldsymbol{x}), \tag{1}$$

where $\boldsymbol{a}^{(j)}$, $j=1,2,3$, are the lattice vectors spanning a lattice Λ (the torus is given by $\mathrm{T}^3 = R^3/\Lambda$). A consistency ("cocycle") condition requires,

$$\Omega_j(\boldsymbol{x}+\boldsymbol{a}^{(k)}) \Omega_k(\boldsymbol{x}) = \exp(i2\pi n_{jk}/N) \Omega_k(\boldsymbol{x}+\boldsymbol{a}^{(j)}) \Omega_j(\boldsymbol{x}), \tag{2}$$

where the element of the center of the group SU(N) (present because of the absence of fields in the fundamental representation) labels the quantized magnetic flux,

$$m_i = \tfrac{1}{2}\varepsilon_{ijk} n_{jk}\,, \tag{3}$$

which is a Z_N vector, i.e. m_i is integer modulo N. One can always choose a gauge where the gauge functions ("cocycles") $\Omega_j(\boldsymbol{x})$ are coordinate independent, leaving a local gauge invariance $\Omega(\boldsymbol{x})$ such that the cocycles $\Omega_j(\boldsymbol{x})$, $(j = 1,2,3)$ remain invariant (see sect. 6).

There are severe problems with the Savvidy state since it is unstable for arbitrary weak background fields. One instability is removed by exciting the unstable mode, but it is not clear whether the resulting ϑ_3 state suffers from further instabilities [10]. Modulo these problems, however, the Savvidy and Copenhagen vacua do provide examples of states with an energy density lower than the perturbative vacuum.

In our approach, we are so far not able to demonstrate any instability of the perturbative vacuum, but we shall argue that further work along these lines might succeed in doing so. The great advantage of our method is that the states we consider, i.e. SU(2) Yang-Mills theory on a torus, or equivalently, a periodic array of Z_2 magnetic fluxes filling all space, are free from instabilities and amenable to rigorous analytical methods. Instead of varying the background magnetic field, we use the size L of the torus as an expansion parameter. (This was discussed in detail for zero magnetic flux in ref. [11b].) For small L, perturbation theory [12] (including tunneling effects [11]) can be used and allows us to study the physics as a function of L and compare with Monte Carlo results. This, we believe, is also the appropriate method for demonstrating chromomagnetic instabilities.

3. The vacuum energy to one-loop

It is clear that $A_k = 0$ satisfies any of the boundary conditions of eq. (1) for constant Ω_j and zero classical energy [13] $V(A) = \frac{1}{2}\int d^3x\, \mathrm{Tr}[F_{jk}^2(\boldsymbol{x})]$. The energy associated to the presence of magnetic flux consequently resembles a Casimir energy in being purely quantum mechanical in origin. For nonzero magnetic flux, $\boldsymbol{m}$, we use Feynman gauge* and have the standard gauge fixed lagrangian, with ghost field ψ. In a gauge where all Ω_j are constant, the boundary conditions read,

$$A_\mu(\boldsymbol{x} + L\boldsymbol{e}_k) = \Omega_k(\boldsymbol{m}) A_\mu(\boldsymbol{x}) \Omega_k^{-1}(\boldsymbol{m})\,, \tag{4a}$$

$$\Psi(\boldsymbol{x} + L\boldsymbol{e}_k) = \Omega_k(\boldsymbol{m}) \Psi(\boldsymbol{x}) \Omega_k^{-1}(\boldsymbol{m})\,, \tag{4b}$$

* For zero magnetic flux a modification will be discussed later.

with

$$\begin{aligned}
\Omega_k(0,0,0) &= \{1_2, 1_2, 1_2\}, \\
\Omega_k(0,0,1) &= \{i\sigma_1, i\sigma_2, 1_2\}, \\
\Omega_k(0,1,1) &= \{i\sigma_1, i\sigma_2, i\sigma_2\}, \\
\Omega_k(1,1,1) &= \{i\sigma_1, i\sigma_2, i\sigma_3\},
\end{aligned} \tag{5}$$

where σ_i are the Pauli matrices. The fluxes $\{(0,0,1),(0,1,0),(1,0,0)\}$ and $\{(0,1,1),(1,0,1),(1,1,0)\}$ are degenerate in energy because of the cubic symmetry.

Expanding the fields in Fourier modes, gives a convenient way of realizing the boundary conditions, eq. (4), in terms of momenta

$$A_\mu = \tfrac{1}{2}\sigma_a A_\mu^a, \qquad A_\mu^a(\boldsymbol{x}) = \sum_{\boldsymbol{k} \in Z^3} A_\mu^a(\boldsymbol{k}) \exp\left(i \frac{2\pi}{L} \left(\boldsymbol{k} + \lambda^{(a)}(\boldsymbol{m}) \right) \cdot \boldsymbol{x} \right), \tag{6a}$$

$$\psi = \tfrac{1}{2}\sigma_a \psi^{(a)}, \qquad \psi^{(a)}(\boldsymbol{x}) = \sum_{\boldsymbol{k} \in Z^3} \psi^{(a)}(\boldsymbol{k}) \exp\left(i \frac{2\pi}{L} \left(\boldsymbol{k} + \lambda^{(a)}(\boldsymbol{m}) \right) \cdot \boldsymbol{x} \right), \tag{6b}$$

with $\lambda^{(a)}(\boldsymbol{m})$ explicitly given by,

$$\begin{aligned}
2\lambda^{(a)}(0,0,0) &= \{(0,0,0),(0,0,0),(0,0,0)\}, \\
2\lambda^{(a)}(0,0,1) &= \{(0,1,0),(1,0,0),(1,1,0)\}, \\
2\lambda^{(a)}(0,1,1) &= \{(0,1,1),(1,0,0),(1,1,1)\}, \\
2\lambda^{(a)}(1,1,1) &= \{(0,1,1),(1,0,1),(1,1,0)\}.
\end{aligned} \tag{6c}$$

We see that for $\boldsymbol{m} \neq \boldsymbol{0}$, color and space-time indices mix, since the translational invariance is realized only modulo a gauge transformation. For SU(N) the situation is slightly more complicated, but choosing an appropriate basis for the Lie algebra dictated by the twist [14], one obtains similar simple results. Note that it is important for consistency that $\Sigma_a (-1)^{n_a} \lambda^{(a)}(\boldsymbol{m})$ is integer for any $\boldsymbol{n} \in Z^3$, which implies that momentum is conserved at the vertices as required by translational invariance.

We have not yet specified the time dependence. If we are only interested in perturbative results, where the electric flux (see sect. 6 for details) plays no role, we can either take continuous timelike momenta, or assume periodicity in time over a distance $t = T$ giving

$$p^{(a)} = \left(\frac{2\pi k_0}{T}, \frac{2\pi}{L}\left(\boldsymbol{k} + \lambda^{(a)}(\boldsymbol{m})\right)\right).$$

It is well known that one can calculate the one-loop effective potential in two ways. Either as a Casimir energy summing up the zero point energies for the individual modes in the harmonic approximation, or by calculating a functional determinant for the inverse propagator after removing the zero eigenvalues. The inverse propagator is just ∂_μ^2, and consequently has a zero mode only for the case of zero magnetic flux. This is the by now well known quartic infrared problem which we will handle by modifying the gauge fixing for $\boldsymbol{m} = \boldsymbol{0}$ as described in detail in ref. [15]. The lowest order one-loop result is, however, not influenced by this and we get

$$E_1(\boldsymbol{m}) = \frac{2\pi}{L} \sum_{a=1}^{3} \sum_{\boldsymbol{k} \in Z^3} \|\boldsymbol{k} + \lambda^{(a)}(\boldsymbol{m})\|. \tag{7}$$

Techniques similar to those employed in ref. [12] give (up to an irrelevant constant),

$$E_1(\boldsymbol{m}) = \frac{1}{2L} \sum_{a=1}^{3} V\left(2\pi\lambda^{(a)}(\boldsymbol{m})\right),$$

$$V(\boldsymbol{C}) = -\frac{2}{\pi^2} \sum_{\boldsymbol{n}=\boldsymbol{0}} \frac{e^{i\boldsymbol{n}\cdot\boldsymbol{C}}}{(\boldsymbol{n}^2)^2} = 2 \sum_{\boldsymbol{k} \in Z^3} \|2\pi\boldsymbol{k} + \boldsymbol{C}\| + \text{const.} \tag{8}$$

The easiest way to evaluate these sums is by using the results of ref. [16] which yields,

$$V(0,0,0) = -2a(4)/\pi^2,$$

$$V(\pi,0,0) = V(0,\pi,0) = V(0,0,\pi) = -2b(4)/\pi^2,$$

$$V(\pi,\pi,0) = V(\pi,0,\pi) = V(0,\pi,\pi) = -2c(4)/\pi^2,$$

$$V(\pi,\pi,\pi) = -2d(4)/\pi^2, \tag{9}$$

where

$$a(2s) = \sum_{\boldsymbol{n}\neq\boldsymbol{0}} \frac{1}{(\boldsymbol{n}^2)^s}, \qquad b(2s) = \sum_{\boldsymbol{n}\neq\boldsymbol{0}} \frac{(-1)^{n_1}}{(\boldsymbol{n}^2)^s},$$

$$c(2s) = \sum_{\boldsymbol{n}\neq\boldsymbol{0}} \frac{(-1)^{n_1+n_2}}{(\boldsymbol{n}^2)^s}, \qquad d(2s) = \sum_{\boldsymbol{n}\neq\boldsymbol{0}} \frac{(-1)^{n_1+n_2+n_3}}{(\boldsymbol{n}^2)^s}. \tag{10}$$

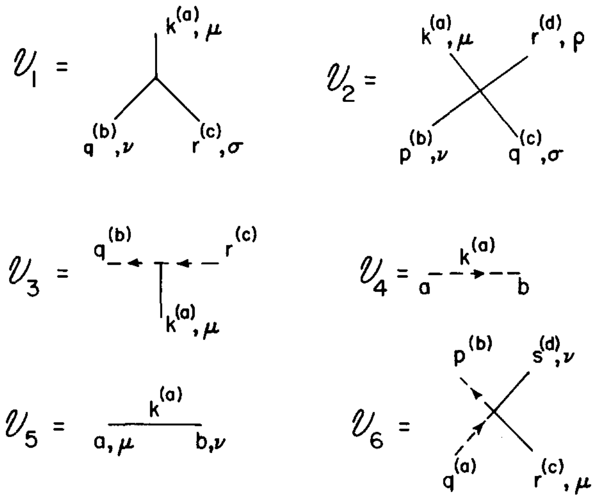

Fig. 1. The graphs for the Feynman rules of eqs. (11) and (23).

4. The two-loop result for $m \neq 0$

Next we calculate the two-loop contribution for $m \neq 0$, where the propagator is not plagued by zero modes. This two-loop result will be proportional to g^2/L. Since the one-loop result is g-independent, the two-loop result should be finite and we need not consider counterterms. The Feynman rules are standard and given in fig. 1 (all momenta are flowing into the vertices) with the $\mathscr{V}_i$ given by

$$\mathscr{V}_1 = g\varepsilon_{abc}\Big[g_{\mu\nu}\big(k_\sigma^{(a)} - q_\sigma^{(b)}\big) + g_{\nu\sigma}\big(q_\mu^{(b)} - r_\mu^{(c)}\big) \\ + g_{\sigma\mu}\big(r_\nu^{(c)} - k_\nu^{(a)}\big)\Big]\delta_4\big(q^{(b)} + k^{(a)} + r^{(c)}\big),$$

$$\mathscr{V}_2 = -ig^2\Big[\varepsilon_{abe}\varepsilon_{cde}\big(g_{\mu\sigma}g_{\nu\rho} - g_{\mu\rho}g_{\nu\sigma}\big) + \varepsilon_{ace}\varepsilon_{bde}\big(g_{\mu\nu}g_{\sigma\rho} - g_{\mu\rho}g_{\nu\sigma}\big) \\ + \varepsilon_{ade}\varepsilon_{cbe}\big(g_{\mu\sigma}g_{\nu\rho} - g_{\mu\nu}g_{\rho\sigma}\big)\Big] \\ \times\delta_4\big(p^{(b)} + k^{(a)} + r^{(d)} + q^{(c)}\big),$$

$$\mathscr{V}_3 = g\varepsilon_{abc}r_\mu^{(c)}\delta_4\big(k^{(a)} + q^{(b)} + r^{(c)}\big),$$

$$\mathscr{V}_4 = \frac{i\delta_{ab}}{\big(k^{(a)}\big)^2 + i\varepsilon},$$

$$\mathscr{V}_5 = \frac{i\delta_{ab}g_{\mu\nu}}{\big(k^{(a)}\big)^2 + i\varepsilon}. \tag{11}$$

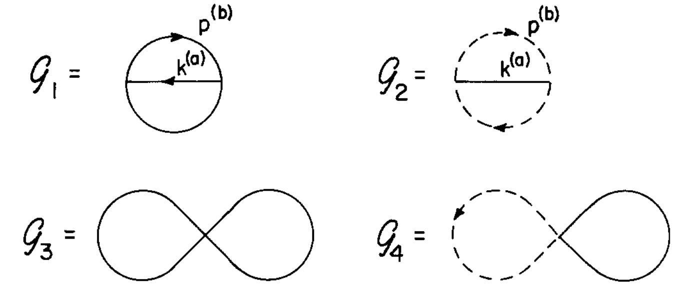

Fig. 2. The graphs for the two-loop diagrams occurring in eqs. (12), (13) and (24).

The two-loop vacuum energy is now the sum of all connected two-loop diagrams*. Since dumbell diagrams give zero (color and/or momentum conservation) we only need to consider one-particle irreducible diagrams. Hence we have (see fig. 2 for the graphs of $\mathcal{G}_i$)

$$E_2(\boldsymbol{m}) = i\left(\tfrac{1}{12}\mathcal{G}_1 - \tfrac{1}{2}\mathcal{G}_2 + \tfrac{1}{8}\mathcal{G}_3\right). \tag{12}$$

Adding the first two diagrams yields,

$$\begin{aligned}\tfrac{1}{12}\mathcal{G}_1 - \tfrac{1}{2}\mathcal{G}_2 &= \frac{-ig^2}{2TL^3}\sum_{k,p}\sum_{a\neq b\neq c}\frac{\left[\left(k^{(a)}+p^{(b)}\right)^2 + \left(p^{(b)}\right)^2 + 2\left(k^{(a)}\right)^2\right]}{\left[\left(k^{(a)}+p^{(b)}\right)^2 + i\varepsilon\right]\left[\left(p^{(b)}\right)^2 + i\varepsilon\right]\left[\left(k^{(a)}\right)^2 + i\varepsilon\right]} \\ &= \frac{-2ig^2}{TL^3}\sum_{a\neq b}\left(\sum_k \frac{1}{\left(k^{(a)}\right)^2 + i\varepsilon}\right)\cdot\left(\sum_p \frac{1}{\left(p^{(b)}\right)^2 + i\varepsilon}\right).\end{aligned} \tag{13}$$

We only performed algebraic manipulations to obtain this result, which is easily seen to be proportional to the last diagram, $\mathcal{G}_3$, in eq. (12). Using the identity

$$\lim_{T\to\infty}\frac{1}{T}\sum_n \frac{1}{(2\pi n/T)^2 - \boldsymbol{k}^2 + i\varepsilon} = \frac{-i}{2\|\boldsymbol{k}\|}, \tag{14}$$

the final result for the two-loop vacuum energy for nonzero magnetic flux is

$$E_2(\boldsymbol{m}) = \frac{g^2}{64L}\sum_{a\neq b} W\left(2\pi\lambda^{(a)}(\boldsymbol{m})\right)W\left(2\pi\lambda^{(b)}(\boldsymbol{m})\right),$$

$$W(\boldsymbol{C}) = 4\sum_{\boldsymbol{k}}\frac{1}{\|2\pi\boldsymbol{k}+\boldsymbol{C}\|} = \frac{2}{\pi^2}\sum_{\boldsymbol{n}\neq\boldsymbol{0}}\frac{e^{i\boldsymbol{n}\cdot\boldsymbol{C}}}{\boldsymbol{n}^2}, \tag{15}$$

* For a similar calculation at finite temperature, see ref. [17].

where $W(2\pi\lambda^{(a)})$ can be obtained from ref. [16] by

$$\begin{aligned}
&W(0,0,0)=2a(2)/\pi^2,\\
&W(\pi,0,0)=W(0,\pi,0)=W(0,0,\pi)=2b(2)/\pi^2,\\
&W(\pi,\pi,0)=W(\pi,0,\pi)=W(0,\pi,\pi)=2c(2)/\pi^2,\\
&W(\pi,\pi,\pi)=2d(2)/\pi^2,
\end{aligned}\tag{16}$$

with $a(2)$, $b(2)$, $c(2)$ and $d(2)$ defined in eq. (10). Note that $W(C)=\partial^2V(C)/\partial C^2$.

5. The two-loop result for $m=0$

Next we discuss the case $m=0$. A naive expansion in Feynman graphs yields an infrared divergence due to the zero momentum states. This problem was carefully studied by Lüscher in a hamiltonian approach [12], and by one of us in a lagrangian approach [11, 15]. The latter is convenient for calculating the vacuum energy in two-loop order. The procedure followed, is to integrate out all spatially nonconstant modes to obtain an effective lagrangian in terms of the spatially constant ones. The vacuum energy is then the ground state energy of the effective hamiltonian obtained from this effective lagrangian. Up to a constant, this effective hamiltonian was determined to one-loop, and to fourth order in the spatially constant vector potentials by Lüscher,

$$H_{\mathrm{eff}}=E^{(0)}(\mathbf{0})+H'.\tag{17}$$

The vacuum energy was calculated (in the MS scheme) by Lüscher and Münster [12] with the following result,

$$L\left(E(\mathbf{0})-E^{(0)}(\mathbf{0})\right)=g^{2/3}\varepsilon_1+g^{4/3}\varepsilon_2+g^2\varepsilon_3+g^{8/3}\varepsilon_4.\tag{18}$$

The higher order terms are influenced by two-loop contributions to H', and only ε_4 in this expression is scheme dependent. Hence, what remains to be determined to fix $E(\mathbf{0})$ to $O(g^{8/3})$ is $E^{(0)}(\mathbf{0})$, which is the vacuum energy for zero external field (i.e. spatially constant vector potentials).

We have already mentioned that $E_1^{(0)}(\mathbf{0})$, is given by eq. (8). Now we will demonstrate that $E_2^{(0)}(\mathbf{0})$, is also given by eq. (15), restricting the sum over $\boldsymbol{k}$ to $\boldsymbol{k}\neq\mathbf{0}$. (This does yield the value of $W(0,0,0)$ given in eq. (16).) Before we review the particular gauge fixing needed for the $m=0$ case, it is obvious that integrating over spatially nonconstant modes leads to the same Feynman rules, except for the constraint $\boldsymbol{k} \neq \mathbf{0}$ in the propagator and a possible nonlocal interaction [15]. The contribution to $E_2^{(0)}(\mathbf{0})$ due to local interactions is still given by the diagrams of eq. (12), except that now one has the constraint $\boldsymbol{k} \neq \mathbf{0}$, $\boldsymbol{p} \neq \mathbf{0}$, and $\boldsymbol{k}+\boldsymbol{p} \neq \mathbf{0}$. This means that eq. (13) is not proportional to the last diagram in eq. (12), because that diagram gives eq. (13) with only $\boldsymbol{k} \neq \mathbf{0}$ and $\boldsymbol{p} \neq \mathbf{0}$ as constraints. Therefore we have

$$E_2^{(0)}(\mathbf{0})_{\mathrm{loc}} = \frac{6g^2}{64L} W(\mathbf{0})^2 - \frac{12g^2}{TL^3} \sum_{\substack{k,p \\ \boldsymbol{k}\neq\mathbf{0},\, \boldsymbol{p}\neq\mathbf{0} \\ \boldsymbol{k}+\boldsymbol{p}=\mathbf{0}}} \frac{1}{(k^2+i\varepsilon)} \frac{1}{(p^2+i\varepsilon)} . \tag{19}$$

Since the interactions are local, the nonlocality of the last term is of course due to the nonlocality of the propagator. It would therefore be highly desirable if this term is *exactly* cancelled by a nonlocal interaction. That this indeed happens can be considered as a significant test of our method for dealing with infrared divergences, without breaking gauge invariance. (A similar subtle behaviour should guarantee the Slavnov-Taylor identities to be satisfied identically.)

To appreciate the cancellation we will review the procedure to deal with the spatially constant modes [15]. Let P be the projection on these constant modes, i.e.

$$PA_\mu = \frac{1}{L^3} \int_{\mathrm{T}^3} \mathrm{d}^3x \, A_\mu(\boldsymbol{x}), \tag{20}$$

and introduce the following nonlocal gauge fixing function,

$$\chi = (1-P)\left(\partial_\mu A_\mu + i\left[PA_\mu, A_\mu\right]\right) + \frac{1}{L} PA_0 , \tag{21}$$

which can be viewed as a background gauge [18] where the background field is dynamical and not inert under gauge transformations. In the process of deriving the ghost lagrangian one has to vary PA_μ as well. This mixes spatially nonconstant vector potentials with spatially nonconstant ghost fields, and leads to the following nonlocal ghost interaction (see ref. [15] for details, $Q_\mu = (1-P)A_\mu$),

$$\mathscr{L}_{\mathrm{nonloc}} = 2g^2 \mathrm{Tr}\left(\left[\bar{\psi}, Q_\mu\right] P \left[Q_\mu, \psi\right]\right), \tag{22}$$

which gives the vertex $\mathscr{V}_6$ in fig. 1:

$$\mathscr{V}_6 = -ig^2 g_{\mu\nu} \varepsilon_{ace} \varepsilon_{bde} \delta(p_0 + q_0 + r_0 + s_0) \delta_{\boldsymbol{p}+\boldsymbol{s}} \cdot \delta_{\boldsymbol{q}+\boldsymbol{r}} . \tag{23}$$

This vertex gives a nonzero contribution* to $E_2^{(0)}(\mathbf{0})$

$$E_2^{(0)}(\mathbf{0})_{\text{nonloc}} = -\tfrac{1}{2}i\mathscr{G}_4$$
$$= \frac{12g^2}{TL^3} \sum_{\substack{k,p \\ k\neq 0, p\neq 0 \\ k+p=0}} \frac{1}{(k^2+i\varepsilon)} \frac{1}{(p^2+i\varepsilon)} . \tag{24}$$

Therefore the final result for $E_2^{(0)}(\mathbf{0})$ becomes

$$E_2^{(0)}(\mathbf{0}) = E_2^{(0)}(\mathbf{0})_{\text{loc}} + E_2^{(0)}(\mathbf{0})_{\text{nonloc}} = \frac{3g^2}{32L} W(\mathbf{0})^2 , \tag{25}$$

as promised.

6. Non-perturbative corrections

Putting the one- and two-loop results together and substituting the numerical values for ε_i, a, b, c, and d we find,

$$\begin{aligned} LE(0,0,0) &= -5.025221 + 4.11672g^{2/3} - 1.174516g^{4/3} \\ &\quad +0.186940g^2 - 0.03148g^{8/3} , \\ LE(0,0,1) &= +0.0788727 + 0.00153208g^2 , \\ LE(0,1,1) &= +0.540126 + 0.00759857g^2 , \\ LE(1,1,1) &= +0.655615 + 0.0128930g^2 . \end{aligned} \tag{26}$$

In eq. (26), g is the running coupling constant, which to two-loop order reads,

$$g^2(L) = -\frac{12\pi^2}{11\ln(\Lambda_{\text{MS}}L)} - \frac{612\pi^2}{1331} \frac{\ln(-2\ln(\Lambda_{\text{MS}}L))}{(\ln(\Lambda_{\text{MS}}L))^2} . \tag{27}$$

It is useful to re-express the result in terms of Lüscher's renormalization group invariant scale parameter z defined by [19]

$$\begin{aligned} z &= M_L(0^+)L \\ &= 2.2696390g^{2/3} - 0.7975278g^{4/3} - 0.319g^2 - 0.145g^{8/3} , \end{aligned} \tag{28}$$

* Note the minus sign for the ghost loop, see graph $\mathscr{G}_4$ in fig. 2.

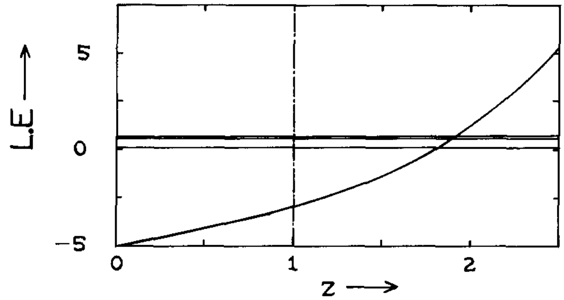

Fig. 3. Behaviour of the vacuum energies versus z as given by eqs. (29).

where $M_L(0^+)$ is the 0^+ glueball mass for zero magnetic flux, and the $g^{2/3}$ expansion is taken from ref. [12b]. We find,

$$\begin{aligned}
LE(0,0,0) &= -5.025221 + 1.813821z + 0.0528137z^2 \\
&\quad + 0.0818z^3 + 0.1097z^4 + \cdots, \\
LE(0,0,1) &= +0.0788727 + 1.310423 \cdot 10^{-4}(z^3 + 1.054169z^4) + \cdots, \\
LE(0,1,1) &= +0.540126 + 6.499225 \cdot 10^{-4}(z^3 + 1.054169z^4) + \cdots, \\
LE(1,1,1) &= +0.655615 + 11.027705 \cdot 10^{-4}(z^3 + 1.054169z^4) + \cdots. \qquad (29)
\end{aligned}$$

These results are shown graphically in fig. 3, where one clearly sees that $LE(\mathbf{0})$ increases much faster than $LE(0,0,1)$. However, the point of crossing will occur beyond $z = 1$, where the perturbative expansion in the zero magnetic flux sector can no longer be trusted due to a tunneling phenomenon described in ref. [11]. This tunneling lifts the degeneracy between states with different electric flux, and in the weak coupling approximation, the perturbative energy is decreased by half the energy of the electric flux (ΔE),

$$\begin{aligned}
LE(0,0,0) &= LE(0,0,0)_{\text{pert}} - \tfrac{1}{2}\Delta E \cdot L, \\
L\Delta E &= 0.00767z^{1/2}\exp(-42.6169z^{-3/2} + 34.2001z^{-1/2})(1 + \cdots). \qquad (30)
\end{aligned}$$

The tunneling was found to set in at $z \sim 1$ (roughly where the exponent changes sign). We have to go beyond a semiclassical approximation to evaluate $LE(\mathbf{0})$ including this tunneling contribution. Since the tunneling can be described in terms of an effective hamiltonian [11, 15], with a finite (6) number of degrees of freedom, a numerical calculation, presently under investigation, is feasible. Moreover, since the tunneling is similar to that of a double well, one expects the ground state energy first to go down (at the point where the tunneling becomes appreciable). At the same time, the ground state energies for tori with nonzero magnetic flux should behave smoothly as a function of z. The latter is expected from the small magnitude of the two-loop contribution as compared with the zero magnetic flux case.

To understand this better, we need to analyze the sources of nonperturbative contributions. This is easily done in the hamiltonian formalism, where we expand around the minimum of the classical potential $V(A)$ to obtain perturbation theory. Even after having removed the homotopically trivial gauge transformations, this minimum is in general not unique. Since the minimum is given by a curvature free potential ($F_{ij}=0$), disconnected minima are related by homotopically nontrivial gauge transformations. Tunneling between these vacua is dominated by nonzero action configurations. On a torus the homotopy is determined by $\boldsymbol{k} \in Z_2^3$ and $\nu \in Z$, i.e. by the twist in the time direction and the winding number respectively. The associated action is [20]

$$S = 8\pi^2 |\nu + \tfrac{1}{2}\boldsymbol{k}\cdot\boldsymbol{m}|. \tag{31}$$

Nonzero action (for all ν) requires $\boldsymbol{k}\cdot\boldsymbol{m} \neq 0 \bmod 2$. This leaves us with those vacua that allow for zero action tunneling. This can only occur if the homotopically nontrivial gauge transformation (necessarily with $\boldsymbol{k}\cdot\boldsymbol{m} = 0 \bmod 2$) has its image point in the same path-connected vacuum component as the original point.

This allows for two possibilities:

(i) There are isolated configurations that are left invariant by homotopically nontrivial gauge transformations. This happens at $\boldsymbol{m} \neq \boldsymbol{0}$.

(ii) There are points that are not fixed under these gauge transformations, in which case the connected components have nonzero dimension. This is realized for $\boldsymbol{m} = \boldsymbol{0}$ and was discussed at great length in previous publications [11, 15]. In this case the vacuum valley acquires an induced potential, which has only isolated minima (one can show that the vacuum valley has points fixed under homotopically nontrivial gauge transformations, but these points correspond to maxima in the induced potential).

The situation is pictorially represented in fig. 4.

Tunneling through a quantum induced barrier sets in much earlier than through a classical potential barrier. The first one has a potential height of $O(g^0)$, the second of $O(g^{-2})$. On the other hand, zero action solutions are also present for $\boldsymbol{m} \neq \boldsymbol{0}$, but are apparently not associated with tunneling since the classical vacuum is isolated. From the fact that this classical vacuum remains fixed under the homotopically nontrivial gauge transformations, it follows that the neighborhood of this vacuum is mapped onto itself and the perturbative wave functionals form representations of

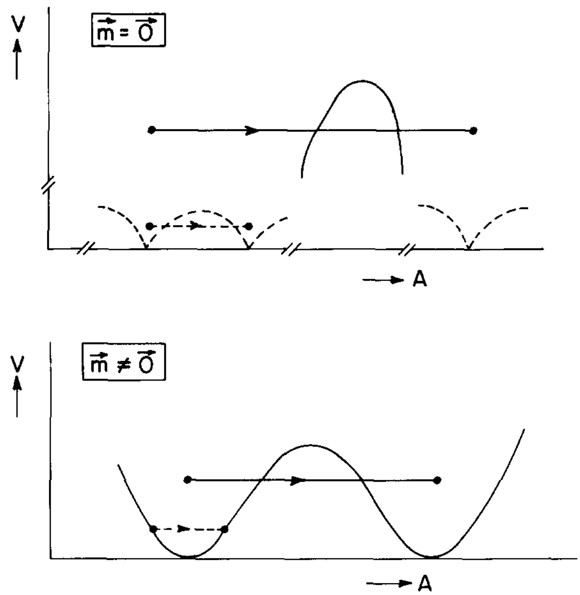

Fig. 4. Schematic representation of the classical potential $V(A)$ for zero and nonzero magnetic flux. The dashed potential for zero magnetic flux is quantum induced. The lines with arrows indicate homotopically nontrivial gauge transformations. For the dashed lines the associated classical action is zero.

the homotopy group of these transformations. The ground state obviously corresponds to the trivial representation.

Let us now be more explicit about these representations (see ref. [21] for an extensive discussion). An allowed gauge transformation satisfies the relation

$$\Omega(x + Le_j) = (-1)^{k_j}\Omega_j\Omega(x)\Omega_j^{-1}, \tag{32}$$

which is equivalent to say that ${}^{\Omega}A$ satisfies the same boundary conditions as A. $\boldsymbol{k} \in Z_2^3$ is the twist in the time direction which (ignoring the winding number [20]) classifies the homotopy group. We will denote a representative of the homotopy group by $\Omega_{\boldsymbol{k}}$. Physical states form representations of this homotopy group and are classified by the electric flux $\boldsymbol{e} \in Z_2^3$,

$$[\Omega_{\boldsymbol{k}}]|\psi_e\rangle = e^{i\pi\boldsymbol{e}\cdot\boldsymbol{k}}|\psi_e\rangle. \tag{33}$$

The gauge transformations $U_{\boldsymbol{k}}$, which leave the vacuum $A = 0$ invariant, are clearly constant and satisfy,

$$U_{\boldsymbol{k}} = (-1)^{k_j}\Omega_j U_{\boldsymbol{k}}\Omega_j^{-1}. \tag{34}$$

It is well known that this equation has solutions iff $\boldsymbol{k}\cdot\boldsymbol{m} = 0 \bmod 2$, consistent with the zero action requirement. Furthermore, they generate a subgroup $S_{\boldsymbol{m}}$ of the

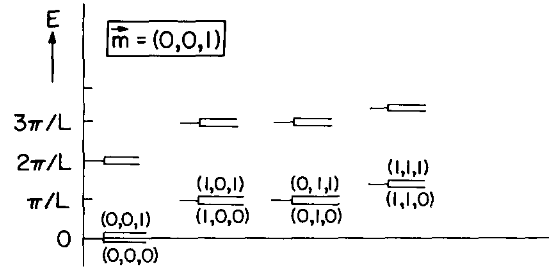

Fig. 5. The low-lying spectrum for magnetic flux (0,0,1). The fine structure due to tunneling, $\Delta E = O(e^{-(4\pi^2/g^2)})$ is not to scale. We have given the electric flux for the lowest levels.

homotopy group, and those representations which are identical when restricted to S_m are degenerate in perturbation theory. To be specific, we will choose $\boldsymbol{m} = (0,0,1)$ (see also ref. [11b]). For this we have $S_m \simeq Z_2^2 = \{\boldsymbol{k} \in Z_2^3 | k_3 = 0\}$ and consequently the electric fluxes which only differ in e_3, will be perturbatively degenerate. The generators of S_m can easily be written down using eq. (4)

$$U_{(0,0,0)} = 1_2 ,$$

$$U_{(1,0,0)} = i\sigma_2 ,$$

$$U_{(0,1,0)} = i\sigma_1 ,$$

$$U_{(1,1,0)} = i\sigma_3 . \tag{35}$$

The action of U_k on the Fourier coefficients in eq. (5) is also easily implemented and translates into multiplication with ± 1.

The spectrum obtained by using the hamiltonian formalism in the Coulomb gauge (compare to ref. [12b]) is depicted in fig. 5, where we normalized to $E(\boldsymbol{e}=\boldsymbol{0}) = 0$. The remaining degeneracy is due to the subgroup of the cubic group O(3, Z) which leaves $\boldsymbol{m}$ fixed, and the first excited state represents the mass gap ($m = 2\pi/L$). The fine structure is due to tunneling, dominated by nonzero action and yields $\Delta E \propto e^{-(4\pi^2/g^2)}$. Similar results hold for the other nonzero magnetic fluxes. Hence we find for nonzero magnetic flux, energies of electric flux and glueball masses proportional to $1/L$ [11b].

In conclusion we have established that for $\boldsymbol{m} \neq \boldsymbol{0}$ and $\boldsymbol{e} = \boldsymbol{0}$ the ground state energy gets a nonperturbative contribution due to tunneling associated with nonzero action solutions and can hence be fully ignored in the region where the tunneling becomes significant for $\boldsymbol{m} = \boldsymbol{0}$. It is therefore likely that we can settle whether any "level crossing" occurs within the context of a perturbative calculation (i.e. using the perturbative expression for the effective hamiltonian to calculate the vacuum energy for $\boldsymbol{m} = \mathbf{0}$ beyond the semiclassical approximation).

The issue of level crossing can also be analyzed numerically by means of Monte Carlo methods, using lattices elongated along the temporal direction. The twisted boundary condition in the short, or spacial, directions can be imposed as described in ref. [22]. Monte Carlo calculations for symmetric lattices and nonzero twists have been performed a long time ago [23], whereas elongated lattices were employed recently in the zero magnetic flux sector [24].

7. Discussion

In this section, we discuss how to rigorously demonstrate the presence of instabilities in the perturbative vacuum, and make some speculations about the nature of the QCD ground state.

First, if a level crossing (of the type discussed at the end of the preceding paragraph) occurs, then there is a possibility that it is energetically favourable for a box with $\boldsymbol{m} = \mathbf{0}$ to "split" into two boxes with $\boldsymbol{m} \neq \mathbf{0}$ by self-imposing suitable boundary conditions. It is an open question whether or not this will occur at a z value where our calculational methods are applicable (we also need to extend our analysis to asymmetric tori). If, however, this happens, we will have an unambiguous demonstration of the instability of the perturbative $\boldsymbol{m} = \mathbf{0}$ vacuum for a torus.

Any speculation about the real QCD vacuum is of course much more dangerous. We can only calculate energy *differences* between periodic structures with different Z_2 magnetic fluxes, but we have no way to demonstrate that such states should be favoured to start with*. In spite of this we shall end with few comments and speculations about the QCD ground state.

Hopefully, it was made clear in the previous section that it is important to get a good understanding of the various tunneling contributions. Besides the analytically well understood Z_2 symmetry restoring transition around $z = 1$, ref. [11b] also presented some numerical evidence for a transition around $z = 4.6$. We will now give three arguments in favour for such a second transition, where the region beyond $z = 4.6$ will be assumed to be the confining phase. This has clear implications for the chromomagnetic instability as discussed below.

The first argument was given in ref. [11b] and is based on the Nambu-Goto string which supposedly describes the long distance features of QCD, but which necessarily breaks down around $z \simeq 4.6$, due to the tachyon [25].

The second reason, is based on finite temperature intuition, which suggests that a deconfining transition should occur when one of the space-time directions become short. If we then simply take $L = 1/T_c$ as the size where a similar transition should occur in our finite volume calculations, we again obtain $z = M(0^+)/T_c \simeq 4.6$. For

* This would amount to prove that self-imposition of (twisted) periodic boundary conditions would be dynamically favoured.

this we have used $\sqrt{\sigma}/M(0^+) = 0.3$ [26,27] and $T_c/\sqrt{\sigma} = 0.74$ [27,28]*. Since much of the finite temperature intuition is based on the absolute value of the Polyakov loop $W_t = \frac{1}{2}|\mathrm{Tr}[i\int_0^T \mathrm{d}t A_0(t)]|$, it is worthwhile to point out how its analogue in the finite volume case, $W_s = \frac{1}{2}|\mathrm{Tr}[i\int_0^L \mathrm{d}x A_1(x)]|$ behaves. Obviously one has $\langle W_s \rangle \simeq 1$ for $z \leq 1$, whereas for $z \geq 4.6$ (assuming this to be the confining region) $\langle W_s \rangle \simeq 0$. However, although it changes rapidly around $z = 1$ (and possibly around $z = 4.6$) there is a continuous and smooth behaviour in between these values. This whole region is therefore absent in the finite temperature analogue $\langle W_t \rangle$, which will be roughly one for $T > T_c$ and zero for $T < T_c$.

The third reason for a second transition is based on the assumption that nonzero action tunneling should be "visible" in graphs of physical quantities as a function of z. Since such nonzero action tunneling sets in so much later than the quantum induced one, $z = 4.6$ could be a likely candidate.

In the light of the above observations, we will end with some speculations. We expect the formation of vacuum domains to be associated with a transition driven by chromomagnetic instabilities at $z \simeq 1$. For the same arguments as in the original Copenhagen vacuum [7], we also need a transition to a "liquid" phase (this among other things restores rotational invariance), which is assumed to be confining. It is tempting to identify the transition at $z = 4.6$ discussed above, with the "melting" of the chromomagnetic domain structure. Of course, we cannot at this point rule out other scenarios. For example, the domain formation could coincide with the transition to the "liquid" phase, in which case it is doubtful whether the picture is of any use at all.

Having said this, let us now discuss the possible nature of the domains. The simplest possibility is that the domains which "melt" are just the Z_2 fluxes discussed earlier. However, large N_c studies [30] and the approximate scaling of the adjoint string tension at moderate distances [31] indicate that objects with nontrivial Z_N structure are not relevant for understanding the confining region. Thus it is quite possible that the domains carry no net magnetic flux, but rather are bound states of N (or a multiple of N) magnetic fluxes. Hence, for SU(2) we might think in terms of magnetic dipole formation. The presence of an instability of the perturbative torus vacuum against splitting, as discussed above, could be an indication of formation of such magnetically neutral domains.

We thank Janos Polonyi for discussions and P.v.B. acknowledges a fruitful interaction with Andreas Gocksch, Julius Kuti and Apoorva Patel, on the nature of the deconfining transition. We are especially grateful to Jeff Greensite for sharing his insights about confinement and offering us valuable criticism.

* That these two different arguments give the same value for z, underlines the relevance of the string picture in the description of the finite temperature phase transitions for SU(2) gauge theory [25,29].

References

[1] E.V. Shuryak, Phys. Reports 115 (1984) 151
[2] S. Mandelstam, Phys. Rev. D19 (1979) 2391;
J. Greensite and M.B. Halpern, Nucl. Phys. B271 (1986) 379;
R. Feynman, Nucl. Phys. B188 (1981) 479
[3] C.G. Callan, R. Dashen, and D.J. Gross, Phys. Rev. D17 (1978), 2717; D19 (1979), 1826
[4] G. 't Hooft, Phys. Scr. 25 (1982) 133;
V.P. Nair and C. Rosenzweig, Phys. Rev. D31 (1984) 401
[5] G.K. Savvidy, Phys. Lett. 71B (1977) 133;
S.G. Matinyan and G.K. Savvidy, Nucl. Phys. B134 (1978) 539
[6] T.H. Hansson, K. Johnson and C. Peterson, Phys. Rev. D26 (1982) 2069
[7] N.K. Nielsen and P. Olesen, Nucl. Phys. B144 (1978) 376;
P. Olesen, Phys. Scr. 23 (1981) 1000;
H. Flyvbjerg, Nucl. Phys. B197 (1982) 155
[8] G. 't Hooft, Nucl. Phys. B153 (1979) 141
[9] J. Ambjørn and P. Olesen, Nucl. Phys. B170 (1980) 265;
J. Ambjørn, B. Felsager and P. Olesen, Nucl. Phys. B175 (1980) 349
[10] L. Maiani, G. Martinelli, G.C. Rossi and M. Testa, Nucl. Phys. B273 (1986) 275
[11a] P. van Baal, Nucl. Phys. B264 (1986) 548
[11b] J. Koller and P. van Baal, Nucl. Phys. B273 (1986) 387
[12a] M. Lüscher, Nucl. Phys. B219 (1983) 233
[12b] M. Lüscher and G. Münster, Nucl. Phys. B232 (1984) 445
[13] J. Ambjørn and H. Flyvbjerg, Phys. Lett. 97B (1980) 241
[14] A. Gonzalez-Arroyo and M. Okawa, Phys. Rev. D27 (1983) 2397;
F. Klinkhamer and P. van Baal, Nucl. Phys. B237 (1984) 274
[15] P. van Baal and J. Koller, Ann. Phys. (NY) 174 (1987) 299
[16] I. Zucker, J. Phys. A8 (1975) 1734
[17] R. Anishetty, J. Phys. G10 (1984) 423
[18] G. 't Hooft, Nucl. Phys. B62 (1973) 444
[19] M. Lüscher, Phys. Lett. 118B (1982) 391
[20] G. 't Hooft, Acta. Phys. Aust. Suppl. 22 (1982) 531;
P. van Baal, Commun. Math. Phys. 85 (1982) 529
[21] P. van Baal, Twisted boundary conditions: ..., thesis, Utrecht (July 1984)
[22] J. Groeneveld, J. Jurkiewicz and C.P. Korthals Altes, Phys. Scr. 23 (1981) 1022
[23] G. Mack and E. Pietarinen, Phys. Lett. 94B (1980) 397
[24] B. Berg and A. Billoire, Phys. Lett. 166B (1986) 203;
B. Berg, A. Billoire and C. Vohwinkel, Phys. Rev. Lett. 57 (1986) 400
[25] P. Olesen, Phys. Lett. 160B (1985) 408
[26] B. Berg, *in* Progress in gauge field theory, Cargese 1983, ed. G. 't Hooft et al. (Plenum, New York 1984)
[27] F. Karsch and C.B. Lang, Phys. Lett. 138B (1984) 176;
J. Ambjørn, P. Olesen and C. Peterson, Nucl. Phys. B240 (1984) 189;
F. Gutbrod and I. Montvay, Phys. Lett. 136B (1984) 411
[28] J. Engels, F. Karsch, H. Satz and I. Montvay, Nucl. Phys. B220 (1983) 223;
G. Gurci and R. Tripicioni, Phys. Lett. 151B (1985) 145
[29] R.D. Pisarski and O. Alvarez, Phys. Rev. D26 (1982) 3735
[30] J. Greensite, Nucl. Phys. B249 (1985) 263;
J. Greensite and M.B. Halpern, Phys. Rev. D27 (1983) 2545;
P. van Baal, Phys. Lett. 140B (1984) 375
[31] P. Olesen, *in* Quark confinement and liberation, eds. F.R. Klinkhamer and M.B. Halpern (World Scientific, Singapore, 1985)